Bioorganic & Medicinal Chemistry 20 (2012) 2549–2557

Contents lists available at SciVerse ScienceDirect

Bioorganic & Medicinal Chemistry

journal homepage: www.elsevier.com/locate/bmc

Synthesis and comparative assessment of a labeled RGD peptide bearing two different ^{99m}Tc-tricarbonyl chelators for potential use as targeted radiopharmaceutical

Dimitrios Psimadas [a,†,*], Melpomeni Fani [a,‡], Eleni Gourni [a,§], George Loudos [b], Stavros Xanthopoulos [a], Christos Zikos [a], Penelope Bouziotis [a], Alexandra D. Varvarigou [a]

[a] Institute of Radioisotopes-Radiodiagnostic Products, N.C.S.R. 'Demokritos', 15310 Aghia Paraskevi, Greece
[b] Department of Medical Instruments Technology, Technological Educational Institute of Athens, Aghiou Spyridonos 28, 12210 Egaleo, Greece

ARTICLE INFO

Article history:
Received 8 January 2012
Revised 20 February 2012
Accepted 22 February 2012
Available online 3 March 2012

Keywords:
RGD
Integrin
Technetium
Radiolabeling
Chelator
Radiopharmaceutical

ABSTRACT

During the past decade radiolabeled RGD-peptides have been extensively studied to develop site-directed targeting vectors for integrins. Integrins are heterodimeric cell-surface adhesion receptors, which are upregulated in cancer cells and neovasculature during tumor angiogenesis and recognize the RGD aminoacid sequence. In the present study, we report the synthesis and development of two derivatives of the Nε-Lys derivatized cyclic Arg-Gly-Asp-D-Phe-Lys peptide, namely of cRGDfKHis and cRGDfK-CPA (CPA: 3-L-Cysteine Propionic Acid), radiolabeled via the $[^{99m}Tc(H_2O)_3(CO)_3]^+$ metal aquaion at a high yield even at low concentrations of 10–5 M (>87%) for cRGDfK-10–5 M (>93%) for cRGDfK-CPA. Radiolabeled peptides were characterized with regard to their stability in saline, in His/Cys solutions, as well as in plasma, serum and tissue homogenates and were found to be practically stable. Internalization and efflux assays using αvβ3-receptor-positive MDA-MB 435 breast cancer cells showed a good percentage of quick internalization (29.1 ± 9.8% for ^{99m}Tc-HiscRGDfK and 37.0 ± 0.7% for ^{99m}Tc-CPA-cRGDfK at 15 min) and no retention of radioactivity for both derivatives. Their in vivo behavior was assessed in normal mice and pathological SCID mice bearing MDA-MB 435 αvβ3 positive breast tumors. Both presented fast blood clearance and elimination via both the urinary and hepatobiliary systems, with ^{99m}Tc-His-cRGDfK remaining for a longer time than ^{99m}Tc-CPA-cRGDfK in all organs examined. Tumor uptake 30 min pi was higher for ^{99m}Tc-CPAcRGDfK (4.2 ± 1.5% ID/g) than for ^{99m}Tc-His-cRGDfK (2.8 ± 1.5% ID/g). Dynamic scintigraphic studies showed that the tumor could be visualized better between 15 and 45 min pi for both radiolabeled compounds but low delineation occurred due to high abdominal background. It was finally noticed that the accumulated activity on the tumor site was depended on the size of the experimental tumor; the smaller the size, the higher was the radioactivity concentration.

1. Introduction

Integrins are transmembrane glycoproteins which facilitate attachment of the cell to the extracellular matrix as well as differentiation, proliferation and migration.[1] They consist of two type of chains (α and β), the structure differentiation of which results in many different integrin types. The $\alpha_v\beta_3$ integrin is of particular interest as it is upregulated in tumor neovasculature and in several

Abbreviations: Arg/R, arginine; Asp/D, aspartic acid; Boc, t-butyloxycarbonyl; BSA, bovine serum albumin; CPA, 3-L-cysteine propionic acid; Cys, cysteine; D-Phe/f, D-phenylalanine; DIEA, *N*,*N*-diisopropylethylamine; DIPC, diisopropylcarbamide; DMEM, Dulbecco's modified Eagle medium; DMF, dimethylformamide; EDTA, ethylenediaminetetraacetic acid; ESI-MS, electrospray ionization mass spectrometry; EtOH, ethanol; FBS, fetal bovine serum; Fmoc, 9-fluorenylmethyloxycarbonyl; Gly/G, glycine; HEPES, 4-(2-hydroxyethyl)-1-piperazineethanesulfonic acid; His/H, histidine; HOBt, 1-hydroxybenzotriazole; ID, injected dose; iv, intravenous; Lys/K, lysine; MeOH, methanol; PBS, phosphate buffered saline; pi, postinjection; PET, positron emission tomography; PMSF, phenylmethanesulfonyl fluoride; ROIs, regions of interest; RP/SE-HPLC, reversed-phase/size-exclusion high-performance liquid chromatography; RT, room temperature; SCID, severe combined immunodeficiency disease, SPECT, single photon emission computerized tomography; SPECT, single photon emission computerized tomography; SPPS, solid phase peptide synthesis; TFA, trifluoroacetic acid; TIPS, triisopropylsilane.

* Corresponding author. Tel.: +30 241350 2916; fax: +30 241350 1863.
E-mail address: dpsimad@chem.uoa.gr (D. Psimadas).
† Corresponding author at present address: Department of Nuclear Medicine, University Hospital of Larissa, 41110 Mezourlo, Larissa, Greece.
‡ Present address: Department of Nuclear Medicine, University Hospital Freiburg, Hugstetterstrasse 55, 79106 Freiburg, Germany.
§ Present address: Department of Pharmaceutical Radiochemistry, Technische Universität München, Meissner-Strasse 3, 85748 Garching, Germany.

0968-0896/$ - see front matter © 2012 Elsevier Ltd. All rights reserved.
doi:10.1016/j.bmc.2012.02.051

types of tumor cells, for example, in melanoma[2] and breast cancer,[3] while it is absent in quiescent blood vessels, rendering it a valuable diagnostic tool. Furthermore, an association between expression of $\alpha_v\beta_3$ and relapse-free survival in breast cancer has been reported,[3] suggesting a prognostic value in imaging such receptors. Labeled synthetic peptides, which contain the tripeptide Arg-Gly-Asp (RGD) amino acid sequence, recognize the $\alpha_v\beta_3$ integrin antagonistically and have proven to be successful agents for in vivo imaging of tumor-related angiogenesis.[1,4,5] It has been showed that in particular cyclic RGD pentapeptides have a relatively high affinity for the $\alpha_v\beta_3$ integrin.[6] After being labeled with a variety of radionuclides, RGD peptides have been further studied as potential radiopharmaceuticals for imaging integrin expression with the PET and SPECT techniques and some of them are already in clinical studies.[7–13]

The γ-emitting nuclide ^{99m}Tc is the preferred radionuclide in diagnostic nuclear medicine for scintigraphy and SPECT imaging, because of its physical decay characteristics ($t_{1/2}$ = 6 h, Ec = 140 keV), its wide availability through commercially-available generator systems and its low cost. The initial development of a low pressure method and the later introduction of a single-vial freeze-dried kit (Isolink®) for the preparation of the $[^{99m}Tc(H_2O)_3(CO)_3]^+$ synthon,[14] boosted the organometallic chemistry of technetium and rhenium in the last decade. The three synthon's aqua ligands are labile and readily substituted by a variety of functional groups (e.g., amines, thiols, carboxylates etc) to give stable complexes.[15–17] Furthermore, the small size and kinetic inertness of the $[^{99m}Tc^{I}(CO)_3]^+$ core make it suitable for the labeling of receptor-targeting molecules.[18–21] The labeling of such biomolecules usually requires the use of a bifunctional chelating agent (BFCA), which on one hand binds to the metal and on the other hand holds the receptor-targeting organic molecules that will render specificity to the complex.

Most ^{99m}Tc studies with RGD peptides up to now have employed the hydrazinonicotinic chelator (HYNIC).[22–27] HYNIC satisfies only part of the coordination requirements of ^{99m}Tc, and additional coligands (e.g., tricine, phosphines) must be incorporated to complete the coordination sphere resulting in bulky and highly charged ^{99m}Tc-complexes. In the following work, we describe the synthesis of a cyclic RGDfK peptide which is conjugated with two different chelators for the tricarbonyl core via the N^{ε} of Lys: His, which acts in a bidentate manner and CPA, which acts in a tridentate manner (Fig. 1). Both derivatives were radiolabeled via the precursor $[^{99m}Tc(H_2O)_3(CO)_3]^+$. In vitro studies were performed to determine the internalization efficiency of the complexes and the degree of residualization of radioactivity into cancer cells, which over-express the $\alpha_v\beta_3$ receptors (MDA-MB 435 human breast cancer cell line[28]), as a function of time. The in vitro/ex vivo stability of both radiolabeled derivatives, as well as their in vivo behavior in normal mice were investigated. Additionally, biodistribution and scintigraphic studies were performed in mice bearing $\alpha_v\beta_3$–positive tumors, in order to evaluate the potential use of the new radiopeptides, as tumor imaging agents in nuclear medicine.

2. Materials and methods

All chemicals were of reagent grade, commercially-available and used without further purification. Side chain protected amino acids were bought from Chemical and Biopharmaceutical Laboratories—Patras, Greece. Technetium-99m, in the form of $^{99m}NaTcO_4$ in saline, was eluted from a commercial ^{99}Mo-^{99m}Tc generator (Mallinckdrodt Medical B.V.). The cancer cell line used in this study was the human MDA-MB 435 breast cancer cell line (NCI, Frederick, Maryland, USA). ESI-MS analysis was performed on a Finnigan AQA Navigator, using a Harvant syringe pump. Radioactivity measurements were conducted in an automated well-typed γ-counter NaI(Tl) crystal (Packard). Female normal Swiss and SCID mice (average weight of 20–25 g) of the same colony and age (approximately 6 weeks) were purchased from the Breeding Facilities of NCSR 'Demokritos'.

2.1. Synthesis of RGD derivatives

Synthesis of the peptide amide was carried out manually by using Fmoc amino acids on an inhouse prepared trityl-type resin, namely 2-Cl-tritylamidomethyl polystyrene resin,[29] following the Fmoc SPPS method. Couplings were performed by using the DIPC/HOBt methology in DMF. Briefly, a fourfold excess of Fmoc-protected amino acid and HOBt were dissolved in DMF (0.2 M). The solution was cooled on ice, and then a fourfold excess DIPC was added. The reaction mixture was initially incubated on ice for 10 min and then at RT for 10 more min at RT. After these two steps it was finally added to the resin (except from the Gly which is added directly to the resin after the first incubation on ice). Coupling efficiency was checked by the Kaiser ninhydrin test. Deprotection of the Fmoc group was achieved by repetitive treatment with 20% piperidine in DMF (3 × 10 min). Cyclisation was performed following a published protocol.[30] Afterwards, the Dde

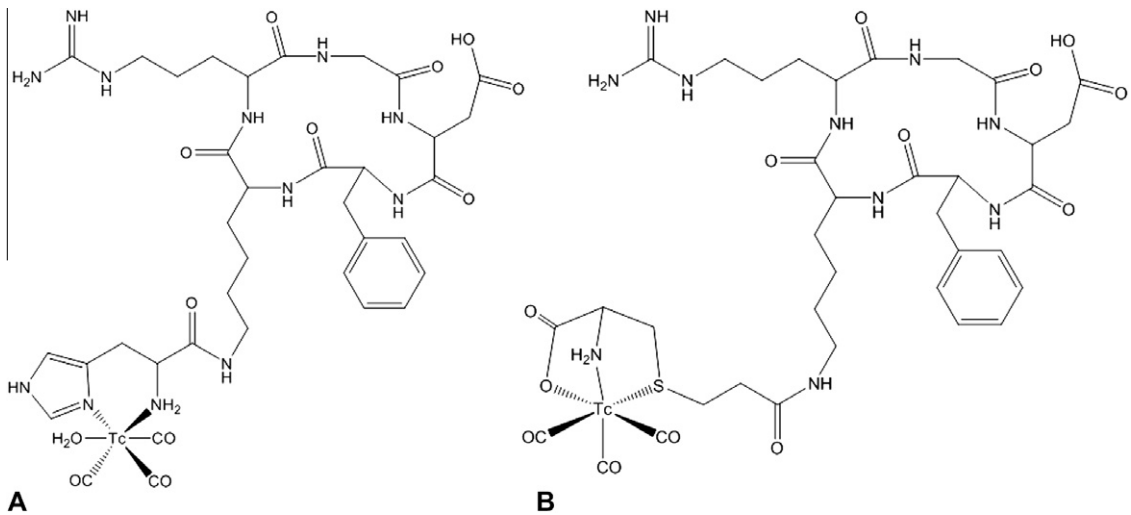

Figure 1. Radiochemical structures of: (A) ^{99m}Tc-His-cRGDfK and (B) ^{99m}Tc-CPA-cRGDfK.

group was removed from the N^{ε}-group of Lys by repetitive treatment with 2% hydrazine in DMF (3 × 3 min). Then the resin was washed with DMF (6×), DCM (6×) and petroleum ether (2×), dried under vacuum and separated in two parts in order to perform the functionalization of the cyclic peptide with the chelators His and CPA. A fourfold excess of 3-iodine propionic acid was dissolved in DCM (0.2 M) and a fourfold excess DIPC was added. The mixture was allowed to react for 15 min at RT and finally added to the resin. After 1 h stirring the resin was washed with DCM (6×) and DMF (6×). A fourfold excess of Boc-Cys-OCH_3 was dissolved in DMF (0.2 M). Afterwards DIEA (fourfold excess) was added and then the mixture was added to the resin and left for 12 h at 25 °C. Then the resin was efficiently washed with DMF (6×), DCM (6×), petroleum ether (2×) and dried under vacuum for 24 h. Coupling of the Fmoc-His-OH to the second part of the resin and then Fmoc deprotection was performed following the same protocol with the other Fmoc-aminoacids mentioned above. This second resin part was efficiently washed and dried as the first one. Both resin-bound peptide derivatives were cleaved from the resin using a cocktail mixture of TFA/TIPS/H_2O (95:2.5:2.5) for 1.5 h. After removal of the organic solvents, the crude products were precipitated with cold diethyl ether, centrifuged and dried under vacuum. The crude peptides were dissolved in water and purified by semipreparative RP-HPLC performed on a Waters HPLC System (10 Nucleosil 7 C_{18} column, 250 × 12.7 mm ID, Macherey Nagel). The solvent system consisted of 0.05% TFA in H_2O (solvent A) and 60% AcCN in 40% A (solvent B). Elution was achieved by applying a linear gradient from 0% B to 50% B in 50 min, at a flow rate of 3 mL/min. The quality control of the prepared peptides was performed with analytical RP-HPLC on a Waters HPLC System (LiChrospher RP C_{18} column, 250 × 4 mm ID, 5 mm particle size, Merck). The solvent system consisted of 0.05% TFA in 0.1 M NaCl (solvent A) and 0.05% TFA in CH_3CN (solvent B). Elution was achieved by applying a linear gradient from 100% A to 60% A in 20 min, at a flow rate of 1.0 mL/min. Detection of the peptide was achieved with a variable-multiwavelength detector (220 nm). For the ESI-MS mass spectral analysis of the two pure peptide derivatives a test solution in 50% aqueous ACN was infused into an electrospray interface mass spectrometer at a flow rate of 0.1 mL/min. Negative or positive ion ESI-MS spectra were acquired by adjusting the needle and cone voltages accordingly. Hot nitrogen gas (Dominic-Hunter UHPLCMS-10) was used for desolvation at 170 °C.

2.2. Radiolabeling

Radiolabeling of the RGD peptide derivatives was performed according to an already published method with slight modifications.[21] Briefly, 225 μL (74–222 MBq) of freshly prepared $[^{99m}Tc(H_2O)_3(CO)_3]^+$ were added in a vial containing 25 μL of cRGDfK-His/CPA peptide solution of various concentrations (from 10^{-3} to 10^{-7} M). The vial was sealed and the mixture was stirred and incubated at 75–80 °C for 20 min. After cooling to RT, radiochemical control was performed on a Waters HPLC System, (μ-Bondapak C_{18} column, 3.9 × 50 mm ID, Waters) applying a linear gradient system at a 1 mL/min flow rate from 100% B to 20% B in 30 min (solvent A: 0.1%TFA in MeOH and solvent B: 0.1% TFA in H_2O). The structure of the two radiolabeled derivatives is presented in Fig. 1.

2.3. In vitro stability studies

The stability of both radiolabeled derivatives was studied by His and Cys challenge. Aliquots of 50 μL of each of the radiolabeled compounds (initial radiolabeling concentration 10^{-4} M) were added to 450 μL of a 10^{-2} M His and 10^{-2} M Cys solution in saline, respectively. The samples were incubated for 1, 2 and 6 h at 37 °C and analyzed by gradient analytical HPLC following the same conditions as described for the radiochemical control of the radiolabeled peptides.

Additionally, the serum stability of the radiopeptides was tested. One hundred microliters of ^{99m}Tc-CPA-cRGDfK or of ^{99m}Tc-His-cRGDfK, (10^{-4} M), were added respectively in 900 μL of human serum. The mixture was incubated at 37 °C for 1, 2 and 6 h and analyzed by SE-HPLC (TSK-Gel G-2000SW column, 7.8 mm × 30 cm, Tosohaas). The elution was performed using a mixture of phosphate buffer 0.1 M, sodium sulfate 0.1 M and sodium azide 0.05% w/v, at pH 6.7.

Finally, the metabolism in human plasma was investigated. Human blood (~3 mL) was collected in heparinized polypropylene tubes and centrifuged at 5000 rpm at 4 °C for 5 min. Aliquots of the radiopeptides were incubated as above with the plasma sample collected, fractions were withdrawn at 15 and 120 min, mixed with EtOH in a 2:1 EtOH/aliquot v/v and centrifuged at 14000 rpm for 30 min. Supernatants were filtered through Millex GP filters (0.22 μm) and analyzed by RP-HPLC.

2.4. Ex vivo metabolism in liver and kidneys

Female Swiss albino mice were ether sacrificed and liver and kidneys were excised, rapidly rinsed and immersed in ice-cold 50 mM TRIS/0.2 M sucrose buffer, pH 7.4. They were subsequently homogenized with a manual homogenizer for 5 min. The radiopeptides were added in fresh homogenate and incubated at 37 °C for 15, 30, and 60 min. In order to determine enzymatic degradation of the peptides, EtOH in a 2:1 EtOH/aliquot v/v was added and the mixture was centrifuged at 14000 rpm for 30 min. The supernatants were filtered through Millex GP filters (0.22 μm) and analyzed by RP-HPLC as described above, for the detection of metabolites species or released $^{99m}TcO_4^-$.

2.5. Cell culture

The MDA-MB 435 human breast cancer cell line was maintained in Dulbecco's DMEM-high glucose supplemented with 10% FBS, 1% L-Glutamine, 1% penicillin/streptomycin, 1% GlutaMAX. Cells were cultured at 37 °C in a humidified incubator under a 5% CO_2 atmosphere and passaged weekly using a trypsin-EDTA solution.

2.6. Internalization and efflux of ^{99m}Tc-CPA-cRGDfK and ^{99m}Tc-His-cRGDfK

For the in vitro internalization analyses, MDA-MB 435 cells were distributed in six-well plates (10^6 cells per well) and cultured overnight. On the day of the experiment, the medium was removed and the cells were washed with binding buffer of pH 7.4 (DMEM-high glucose supplemented with 1% FBS, 1% L-Glutamine, 1% penicillin/streptomycin, 1% GlutaMAX, 50 mM HEPES, 1 μg/mL aprotinin, 0.25 mM PMSF, and 0.125% BSA). Subsequently, in each well, was added 1.2 mL of internalization medium (DMEM containing 1% FBS) and 150 μL of a PBS/0.5% BSA solution containing $1 \times 10^5 - 3 \times 10^5$ cpm of each radiopeptide. This amount of radioactivity corresponds to 200 fmol of the total peptide (the concentration of the total peptide was kept the same for all internalization experiments). The cells were incubated at 37 °C in 5% CO_2. Internalization was stopped at appropriate time points (5, 15, 30, 60, 90 and 120 min) by removing the medium. The cells were washed twice with ice-cold PBS (pH 7.4) and then were washed twice with 1 mL of Gly buffer (0.05 mM Gly solution, pH adjusted to 2.8 with 1 N HCl) for 5 min at 37 °C to distinguish between cell surface-bound (acid-releasable) and internalized (acid-resistant) radioligand. Finally, cells were solubilized with 1 N NaOH at 37 °C for 10 min to detach them from the plates. Surface-bound and

internalized activities were measured in a γ-counter. Considering that the total activity comprises surface-bound plus internalized activity, the % internalized activity for the different time points was calculated with Microsoft Excel.

Externalization studies of the maximum internalized radioactivity were also performed after a 90 min internalization period. The medium was discarded and the cells were washed three times with cold buffer. New medium was added and the cells were incubated at 37 °C. Sampling at 5, 15, 30, 60, 120 and 180 min post-internalization was performed by an initial cold buffer wash of the cells, followed by acid wash (for removal of surface-bound activity), as previously described, and finally by treatment with 1 N NaOH to extract the radioactivity remaining trapped. Externalized, surface-bound and internalized activities were measured in a γ-counter and calculated as above. All experiments were carried out two to three times in triplicate.

2.7. Animal models

Athymic SCID mice were inoculated subcutaneously into the leg (anterior or posterior) with MDA-MB 435 cells (approximately 10^7 cells / animal) in 100 μL of medium . Tumors were allowed to grow for 3 weeks (tumor weight reached 0.1 to 1.2 g) and the animals were used for biodistribution and imaging studies. All animal experiments were performed in compliance with the European legislation for animal welfare. All animal protocols have been approved by the Greek Authorities.

2.8. Biodistribution studies in normal and tumor bearing mice

The in vivo behavior of ^{99m}Tc-CPA-cRGDfK and ^{99m}Tc-His-cRGDfK was studied by iv administration via the tail vein of 100 μL (4–7 MBq) of each radiopeptide per animal. Animals were sacrificed by ether anesthesia, and the main organs were removed, weighed, and counted, together with samples of blood, muscle and urine, in a γ-counter system. Results were expressed as %ID per organ and per gram of each organ/tissue, in comparison to a standard of the injected solution. Stomach and intestines were not emptied before the measurements. For total blood radioactivity calculation, blood is assumed to be 7% of the total body weight.[31] Biodistribution data are given as percent injected dose per gram of tissue (% ID/g) and are means ± SD (n = 3–5).

2.9. Dynamic imaging studies in tumor bearing mice

For dynamic imaging studies athymic SCID mice bearing MDA-MB 435 tumors, were injected intravenously via the tail vein with 100 μL (4–7 MBq) of each radiolabeled compound per animal. An initial stock solution of the anesthetic was prepared by dissolving 1.0 g of 2,2,2-tribromomethanol in 1.0 mL of 2-methyl-2-butanol and it was kept in the dark at 4 °C. On the day of the experiment, an amount of 50 μL of the above solution was dissolved in 1 mL of NaCl 0.9%. The animals were subsequently anesthetized by the subcutaneous injection of this solution at a dose of 10 μL/g body weight. At approximately 5 min pi mice were placed on a high resolution gamma camera, which is the ideal position for planar studies. It minimizes distance between the animal and the collimator so that maximum resolution and sensitivity can be achieved. The small mouse-sized camera employed in this study was manufactured by members of our team.[32] It is based on two Position Sensitive Photomultiplier Tubes (H85000, Hamamatsu, Japan), a parallel hole collimator and a NaI:Tl pixilated scintillator. The spatial resolution of the systems is ~1.5 mm at 0 mm distance from the collimator surface. Data were acquired continuously and sequential images of 2 min frames were stored. Using ImageJ software, ROIs were drawn in the region of the tumor, and on a symmetric background region (up left hand). In addition, ROIs were drawn on bladder, as well as on a region covering liver, spleen, bladder, kidneys and intestines; since these organs overlap it is not easy to separate them in planar imaging. The number of counts in each ROI was divided by the number of total counts and percentage of radioactivity per organ was plotted as a function of time post injection.

3. Results and discussion

3.1. Synthesis and characterization of cRGDfK-His/CPA

Synthesis of cRGDfK bearing His and CPA as chelators for the tricarbonyl core was performed following an Fmoc-based SPPS protocol. Crude derivatives of both peptides were obtained after cleavage at a yield of approximately 80%. The chemical purity after purification was higher than 95% for both derivatives, as determined by analytical RP-HPLC (overall yield approximately 45%). They were both characterized by ESI-MS. The molecular masses obtained for cRGDfK-His (740.5 ± 5.4) and cRGDfK-CPA (792.8 ± 6.2) were in accordance with the expected ones, calculated on the basis of each derivative's primary structure (740.7 and 792.9, respectively).

3.2. Radiolabeling and quality control

The purified peptide derivatives were efficiently labeled at high specific activity, using the carbonyl aquaion $[^{99m}Tc(H_2O)_3(CO)_3]^+$ as starting complex. Analysis with RP-HPLC of the reaction mixture revealed a single radioactive species for both derivatives, at a yield higher than 98% (Fig. 2), which remained stable for at least

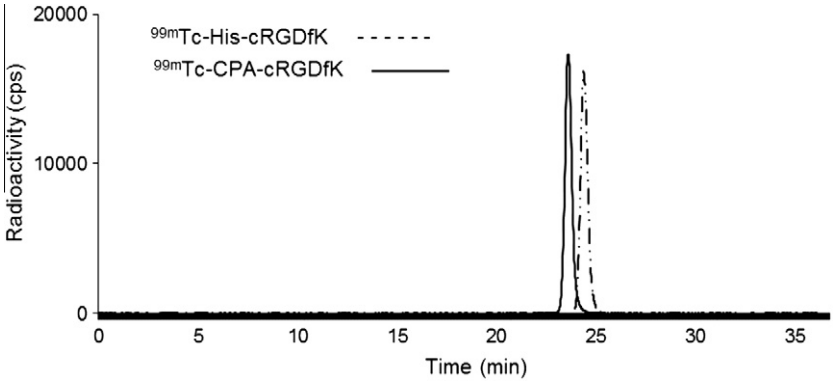

Figure 2. Co-elution RP-HPLC analysis profiles of the two radiolabeled derivatives.

24 h after labeling. The retention times of the two radiopeptides are close [^{99m}Tc-His-cRGDfK: 24.1 min and ^{99m}Tc-CPA-cRGDfK: 23.7 min]. Both peptides could be efficiently radiolabeled even at low concentrations: cRGDfK-His could be labeled at a yield of 95 ± 2% at a concentration of 10^{-5} M, while cRGDfK-CPA could be labeled at a yield of 90 ± 3% even at a concentration of 5.0×10^{-5} M.

3.3. In vitro stability

The in vitro stability study against ligand exchange and/or decomposition, as determined via His and Cys challenge, showed that neither His nor Cys presence (strong competitors for ^{99m}Tc^{I}) led to significant instability. Only insignificant reoxidation of the radionuclide moiety after 6 h incubation was detected, which was 2 ± 1 % in the case of ^{99m}Tc-His-cRGDfK and 9 ± 3 % in the case of ^{99m}Tc-CPA-cRGDfK. High transchelation stability is well known for most ^{99m}Tc-tricarbonyl complexes and it is confirmed here for both chelators used for the peptide labelling.[17,33–35]

Human serum and plasma stability studies were performed to determine whether the functional groups of serum proteins act competitively for the *fac*-[^{99m}Tc(CO)$_3$]-core. Results show that they are both stable in plasma and serum. The only differentiation was that ^{99m}Tc-His-cRGDfK, when incubated with serum, started to decompose already after 1 h (85 ± 2%) remaining practically stable until 6 h (80 ± 2%), while ^{99m}Tc-CPA-cRGDfK did not show any instability at 1 h (<98%), but presented a similar decomposition at 6 h (86 ± 3%) most likely this slight difference cannot be attributed to the disruption of the complex and the transfer of the *fac*-[^{99m}Tc(CO)$_3$]-core to the serum proteins, since the two compounds were very stable in the presence of strong tridentate ligand systems. It can be explained though, through the bidentate way that His complexes Tc^{I} in the cRGDfK-His derivative and by the possible early substitution of the labile H_2O molecule in the ^{99m}Tc-His-cRGDfK complex by functional groups of the serum proteins.[21,33] On the contrary CPA, like all tridentate chelators, presented only low serum binding.[17,21]

3.4. Ex vivo metabolic stability

Stability in kidney and liver homogenates was high (>96%), even after 1 h of incubation (Fig. 3), indicating that no enzymatic degradation occurred for both radiolabeled RGD-derivatives.[18,21] This is a crucial characteristic, which is essential for a radiopharmaceutical, in order for it to present potentiality for clinical application and has also been observed with RGD derivatives labeled with ^{99m}Tc via the HYNIC chelator.[22,23] It is important to note here that radioactivity losses during the procedure (centrifugation and filtration) were minimum and the percentage of radioactivity in the final solution, which was tested by RP-HPLC, was >80% of the initial radioactivity.

3.5. Internalization and efflux analysis

The grade of internalization and efflux as a function of time of the two radiolabeled compounds as a function of time, was assessed in the $\alpha_v\beta_3$-positive MDA-MB 435 human breast cancer cells, at 37 °C. Figure 4 reports the results of this study. It can be observed that within the first 15 min of incubation, the proportion of radioactivity migrating into the cells increased significantly. More specifically, in relation to the cell-associated activity after 15 min of incubation, 29.1 ± 9.8% of ^{99m}Tc-His-cRGDfK and 37.0 ± 0.7% of ^{99m}Tc-CPA-cRGDfK were internalized, attaining a maximum value of approximately 45–50% after 90 min for both derivatives. The internalized percentage remained at this level for 2 h. From the internalization curves of Figure 4 it is concluded that the internalization behavior of the two radiolabeled compounds presented some differences during the first 30 min of incubation, with ^{99m}Tc-CPA-cRGDfK being more rapidly internalized. Gradually, the internalized activity related to the total added presented no substantial difference from one derivative to the other after 90 min of incubation, suggesting thus that the chelator had no significant effect on the cRGDfK internalization properties at late time-points. The rate of internalization of agonists is known to be relatively higher than that of antagonists, such as RGD peptides.[5,20] Nevertheless, the internalization observed in the present study was rather fast and high and this is in accordance with relevant literature.[36,37] A radiopharmaceutical which enters the target-cell is more preferable than one that stays on the cell surface, because its residence time inside the cell is extended, facilitating its imaging and/or therapeutic goal.

The efflux curves of the ^{99m}Tc-complexes are presented in Figure 4. Despite the rapid uptake and the high total amount of internalized radioactivity, there was no long-term retention into the cells, with approximately 50% of the internalized radioactivity being released between 30 and 60 min for both radiopeptides, probably due to the ability of functional intracellular proteases to degrade them. After 3 h that percentage becomes approximately 60%. The rapid radioactivity externalization does not preclude the potential application of these radiolabeled derivatives for diagnostic purposes, because the remaining internalized amount of radioactivity is enough to produce satisfactory images. However, new analogues should be developed for therapeutic applications, with higher retention time into the cells.

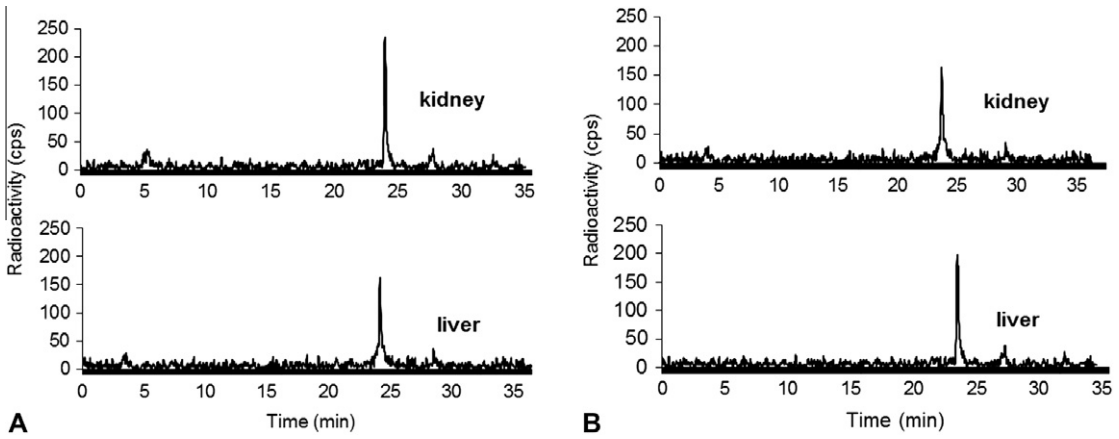

Figure 3. RP-HPLC traces of (A) ^{99m}Tc-His-cRGDfK and (B) ^{99m}Tc-CPA-cRGDfK in liver and kidney homogenates after 1 h incubation at 37 °C.

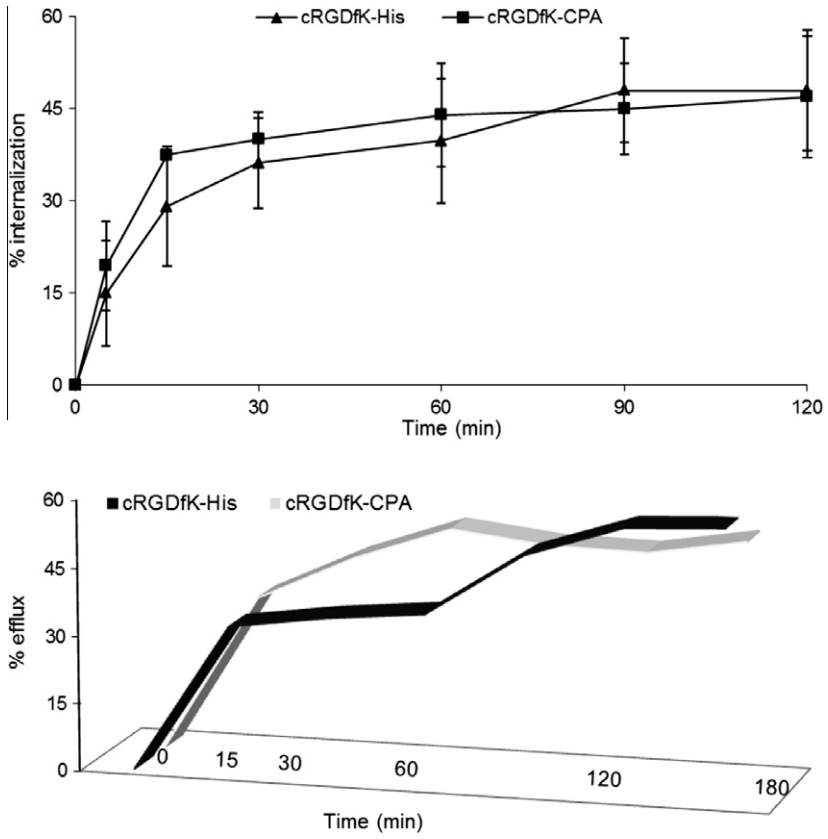

Figure 4. Internalization and efflux curves (after maximum internalization) of the two radiolabeled derivatives. Data represent the percentage of internalized and trapped radioactivity into the cells as well as externalized radioactivity respectively, in relation to the total added radioactivity. Results represent the mean of three experiments.

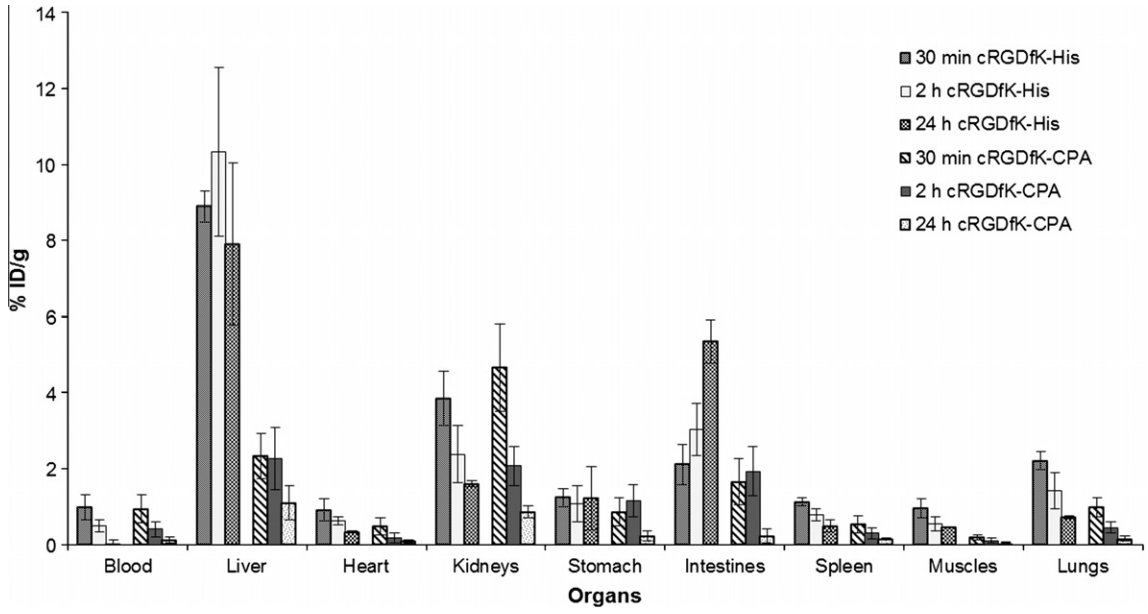

Figure 5. Comparative biodistribution results of ^{99m}Tc-His-cRGDfK and ^{99m}Tc-CPA-cRGDfK in normal mice at 30 min, 2 and 24 h pi (% ID/g). Each value is the average of three animals.

3.6. In vivo characterization with anatomical techniques

The in vivo characterization was initially carried out in normal mice. The biodistribution results of the two derivatives in this species are presented in Figure 5. Rapid blood clearance was observed for both radiopeptides. No significant uptake or retention in the stomach was observed, providing evidence for the stability of the complexes in vivo. The main route of radioactivity clearance was through the kidneys to the urine, as indicated by the high radioactivity concentration in the urine at 30 and 120 min pi (28.5 ± 4.2%

and 20.8 ± 8.4% ID/g for ^{99m}Tc-His-cRGDfK and 23.6 ± 9.3% and 22.8 ± 6.2% ID/g for ^{99m}Tc-CPA-cRGDfK, respectively). Nevertheless, a significant portion of radioactivity showed hepatobiliary clearance, especially in the case of ^{99m}Tc-His-cRGDfK, which presented relatively high liver and intestine accumulated activity even at 24 h pi (7.9 ± 2.1% ID/g and 5.3 ± 0.6% ID/g, respectively). On the contrary, clearance of ^{99m}Tc-CPA-cRGDfK was faster and retention in all organs was lower than 3% ID/g even after 30 min pi (except from the kidneys: 4.7 ± 1.2% ID/g). The above is the only substantial difference between the biodistribution profiles of the two derivatives. It is generally known that not only the binding ability but also the pharmacokinetic properties of a biomolecule, especially of an oligopeptide, can be significantly affected by the chelator which has been used for labeling.[37–39] For example RGD derivatives labeled via the HYNIC approach have shown low liver and intestinal uptake while the kidney uptake, as well as blood retention in some cases, was very high.[23–27] Concerning the relatively high liver and kidney uptake of the radiocompounds, the possibility of transchelation can be safely excluded since ex vivo metabolic stability showed that they remain intact after incubation with liver and kidney homogenates. Previous studies with the lipophilic ^{99m}Tc-tricarbonyl core have indicated that significant liver and kidney uptake can occur with bidentate and not only, coordinated ligands.[17–21,33,40]

Biodistribution studies in SCID mice bearing experimentally induced tumors overexpressing the $\alpha_v\beta_3$ receptors were also performed. Tumor sizes in this study varied from 0.1 to 1.2 g. The values obtained in healthy tissues were comparable to those obtained from normal mice, injected with the same derivative. Maximum tumor uptake was observed at 30 min pi and it was 2.8 ± 1.5% ID/g for ^{99m}Tc-His-cRGDfK and 4.2 ± 1.5% ID/g for ^{99m}Tc-CPA-cRGDfK. Tumor uptake of ^{99m}Tc-CPA-cRGDfK is considered to be high, especially when compared to other ^{99m}Tc-labeled compounds.[23] The tumor to blood (T/bl), tumor to muscle (T/mus) and tumor to liver (T/liv) ratios at 30, 90 and 120 min pi for both radiolabeled derivatives are presented in Figure 6. All tumor to background ratios are higher for ^{99m}Tc-CPA-cRGDfK, due to the higher tumor uptake of this compound compared to ^{99m}Tc-His-cRGDfK at all time-points. The T/liv ratios were <2 for both compounds at any time pi calculated, which may be attributed to the high liver concentration they both present. However, the differences in this case are also in favor of ^{99m}Tc-CPA-cRGDfK. The higher tumor uptake of ^{99m}Tc-CPA-cRGDfK: (a) can be attributed to the different chelator for the tricarbonyl core which probably affects the in vivo binding properties of cRGDfK[38,39,41] and (b) it reflects the higher stability and more rapid internalization rate ofthis compound when compared to ^{99m}Tc-His-cRGDfK (see Sections 3.3 and 3.5). It is important to refer at this point that in ^{99m}Tc-CPA-cRGDfK the propionic acid moiety acts as a spacer between the RGD binding site and the Cys-complex with the tricarbonyl core, providing enhanced binding and pharmacokinetic properties to the overall radiolabeled derivative, while in ^{99m}Tc-His-cRGDfK where there is no distance between the RGD peptide and the ^{99m}Tc-His complex. The T/bl and T/liv ratios measured for the ^{99m}Tc-CPA-cRGDfK derivative are comparable to those measured for ^{99m}Tc-HYNIC labelled compounds while it is important to note that the T/mus ratio is considerably greater.[23] Finally it was studied whether tumor uptake was affected by tumor size and it was found that tumor uptake depended on the size of the tumor, with smaller tumors exhibiting higher radioactivity retention per gram (Fig. 7). The presence of several receptors (e.g., $\alpha_v\beta_3$) is restricted in relatively large tumors because of the presence of hypoxic/necrotic regions within more developed tumors, in which these receptors are expressed less.[41–43] On the other hand RGD peptides are not effective in detecting very small tumors (⩽2 mm), because of their rapid clearance.[38]

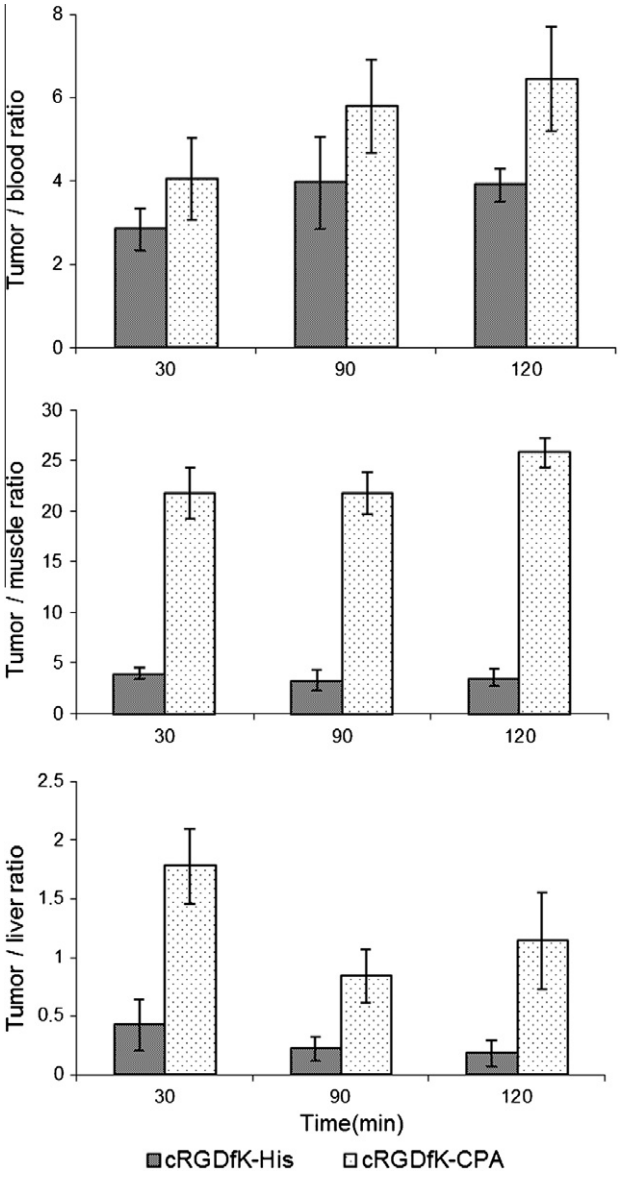

Figure 6. Graphical presentation of the T/bl, T/m and T/liv ratios, at 30, 60 and 120 min pi of the two radiolabeled compounds (n = 3).

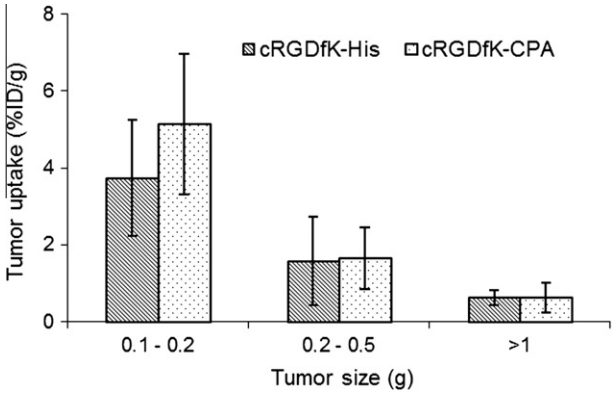

Figure 7. In vivo tumor uptake (% ID/g) at 30 min pi of ^{99m}Tc-His-cRGDfK and ^{99m}Tc-CPA-cRGDfK depending on the tumor size (n = 5).

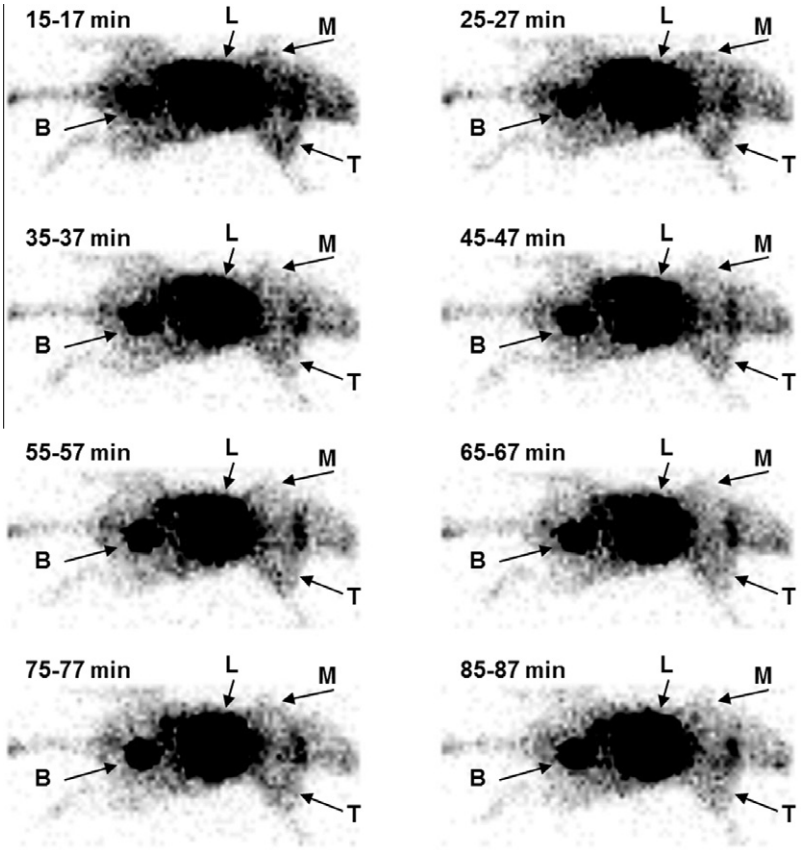

Figure 8. Gamma-ray planar images of a tumor bearing mouse administered with ^{99m}Tc-CPA-cRGDfK; Selected 2-min frames from 15 min up to 87 min pi. Arrows indicate the presence of the tumor (T), liver + spleen + kidneys + intestines (L), muscle (M) and urinary bladder (U).

3.7. Dynamic scintigraphic evaluation

Imaging properties of the radiolabeled derivatives were assessed by dynamic γ-camera images of anaesthetized tumor-bearing mice, from 5 min until approximately 90 min pi (Fig. 8). The data form scintigraphic images were collected, analyzed and evaluated. The in vivo planar imaging studies show that after iv administration, both compounds were rapidly cleared from the blood pool. Concentration of the radiopeptides in the $\alpha_v\beta_3$ positive tumor can be appreciated in both cases; however, the images also show high-level background activity in kidney, liver, and gastrointestinal tract as expected from the biodistribution data. It was found that higher tumor uptake, compared with the rest of the body, was obtained in the period from 15 to 45 min pi for both derivatives. However tumor uptake was maintained until the end of the dynamic imaging session as it was confirmed by the ROI graphs, where the total counts in the tumor region are higher than the background and remain high throughout the experiment (Fig. 9). This suggests that specific radioactivity uptake in the $\alpha_v\beta_3$ rich area of the tumor exists, even though it is not clearly visualized due to the high abdominal concentration that is observed, despite the fact that the tumor was developed far from the abdominal area. This was also observed by Janssen et al. in a study where an RGD derivative was labeled via the HYNIC approach.[26] No blocking or a low expressing cell line was used in the experiments for comparative assessment, because of this high abdominal concentration which does not allow clear imaging of receptor-expressing tumors in the first place. Moreover the MDA-MB 435 breast cancer cells are well defined that they widely express the $\alpha_v\beta_3$ integrin receptors that are recognizable by the RGD motif, hence the binding of the RGD compounds was considered to be specific. The above findings are consistent with already published studies both with RGD peptides and the tricarbonyl core.[19,22,36,44]

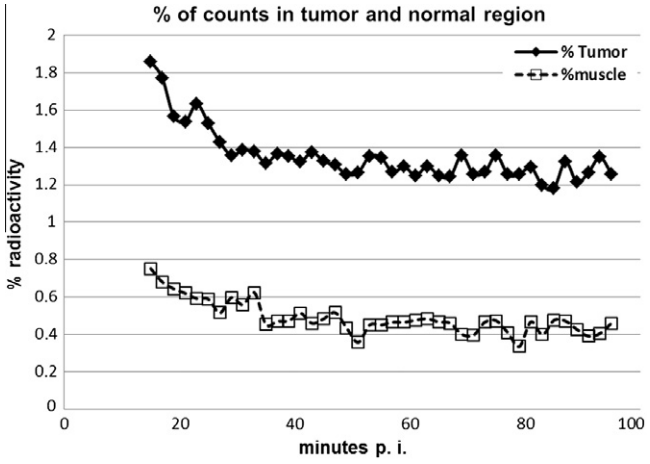

Figure 9. ROI analysis of dynamic imaging after ^{99m}Tc-CPA-cRGDfK administration in tumor leg and opposite normal leg.

4. Conclusion

This work was an attempt to compare two different chelating systems, a bidentate one and a tridentate one, for technetium (I) labeling of a cyclic RGD derivative. We chose to directly compare these two chelating systems in a cell line which over-expresses the $\alpha_v\beta_3$ integrin receptor, namely the MDA-MB 435 breast cancer

cell line. Our results in demonstrated that the incorporation of two different chelators in the cyclic RGDfK peptide has an effect on the in vitro and in vivo properties of the ^{99m}Tc-complexes formed by the radiolabeling with the tricarbonyl core. Both derivatives were labeled in high yields, even at low concentrations, but the one bearing the CPA chelator presents better stability, binding and pharmacokinetic properties in vitro and in vivo. However, imaging applications of both compounds could benefit from reduction of the relatively high abdominal radioactivity levels, most likely due to significant hepatobiliary clearance, in order to obtain a better delineation of the tumor. Further modifications in the structure of the cyclic peptide and/or in the attached bifunctional chelator, which will optimize its pharmacokinetics, can lead to an attractive candidate for the imaging of $\alpha_v\beta_3$ positive tumors labeled via the ^{99m}Tc-tricarbonyl core. Current work is in progress regarding the assessment of the more-promising tridentate chelator slightly modified, in a variety of cancer cell lines with high and low receptor expression.

Acknowledgments

The authors would like to thank Dr. Leondios Leondiadis for ESI-MS analysis performed at the Mass Spectrometry and Dioxin Analysis Lab of NCSR 'Demokritos', Dr. Walter Mier (Department of Nuclear Medicine, University Hospital Heidelberg) for the kind offering of the cell line and Dr. Minas Papadopoulos, Dr. Ioannis Pirmettis and Dr. Theodoros Tsotakos (N.C.S.R. 'Demokritos') for constructive discussion. Financial support was provided by the General Secretariat of Research and Technology grant 'Research in Excellence'.

References and notes

[1]. Folkman, J. *Semin. Cancer Biol.* **2003**, *13*, 159.
[2]. Johnson, J. P. *Cancer Metast. Rev.* **1999**, *18*, 345.
[3]. Gasparini, G.; Brooks, P. C.; Biganzoli, E.; Vermeulen, P. B.; Bonoldi, E.; Dirix, L. Y.; Ranieri, G.; Miceli, R.; Cheresh, D. A. *Clin. Cancer Res.* **1998**, *4*, 2625.
[4]. Haubner, R. *Eur. J. Nucl. Med. Mol. Imaging* **2006**, *33*, S54.
[5]. Hwang, R.; Varner, J. *Hematol. Oncol. Clin. N. Am.* **2004**, *18*, 991.
[6]. Garanger, E.; Boturyn, D.; Dumy, P. *Anticancer Agents Med. Chem.* **2007**, *7*, 552.
[7]. Axelsson, R.; Bach-Gansmo, T.; Castell-Conesa, J.; McParland, B. J. *Study Group Acta Radiol.* **2002**, *51*, 40.
[8]. Beer, A. J.; Schwaiger, M. *Methods Mol. Biol.* **2010**, *680*, 183.
[9]. Decristoforo, C.; Hernandez Gonzalez, I.; Carlsen, J.; Rupprich, M.; Huisman, M.; Virgolini, I.; Wester, H.-J.; Haubner, R. *Eur. J. Nucl. Med. Mol. Imaging* **2008**, *35*, 1507.
[10]. Kenny, L. M.; Coombes, R. C.; Oulie, I.; Contractor, K. B.; Miller, M.; Spinks, T. J.; McParland, B.; Cohen, P. S.; Hui, A. M.; Palmieri, C.; Osman, S.; Glaser, M.; Turton, D.; Al-Nahhas, A.; Aboagye, E. O. *J. Nucl. Med.* **2008**, *49*, 879.
[11]. Mittra, E. S.; Goris, M. L.; Iagaru, A. H.; Kardan, A.; Burton, L.; Berganos, R.; Chang, E.; Liu, S.; Shen, B.; Chin, F. T.; Chen, X.; Gambhir, S. S. *Radiology* **2011**, *260*, 182.
[12]. Schnell, O.; Krebs, B.; Carlsen, J.; Miederer, I.; Goetz, C.; Goldbrunner, R. H.; Wester, H.-J.; Haubner, R.; Pöpperl, G.; Holtmannspötter, M.; Kretzschmar, H. A.; Kessler, H.; Tonn, J. C.; Schwaiger, M.; Beer, A. J. *Neuro-Oncol.* **2009**, *11*, 861.
[13]. Schottelius, M.; Laufer, B.; Kessler, H.; Wester, H.-J. *Acc. Chem. Res.* **2009**, *42*, 969.
[14]. Alberto, R.; Schibli, R.; Egli, A.; Schubiger, A. P.; Abram, U.; Kaden, T. A. *J. Am. Chem. Soc.* **1998**, *120*, 7987.
[15]. Karagiorgou, O.; Patsis, G.; Pelecanou, M.; Raptopoulou, C. P.; Terzis, A.; Siatra-Papastaikoudi, T.; Alberto, R.; Pirmettis, I.; Papadopoulos, M. *Inorg. Chem.* **2005**, *44*, 4118.
[16]. Papagiannopoulou, D.; Tsoukalas, C.; Makris, G.; Raptopoulou, C. P.; Psycharis, V.; Leondiadis, L.; Gniazdowska, E.; Koźmiński, P.; Fuks, L.; Pelecanou, M.; Pirmettis, I.; Papadopoulos, M. S. *Inorg. Chim. Acta* **2011**, *378*, 333.
[17]. Schibli, R.; La Bella, R.; Alberto, R.; Garcia-Garayoa, E.; Ortner, K.; Abram, U.; Schubiger, P. A. *Bioconjug. Chem.* **2000**, *11*, 345.
[18]. Alves, S.; Correia, J. G. D.; Gano, L.; Rold, T. L.; Prasanphanich, A.; Haubner, R.; Rupprich, M.; Alberto, R.; Decristoforo, C.; Santos, I.; Smith, C. J. *Bioconjug. Chem.* **2007**, *18*, 530.
[19]. D'Andrea, L. D.; Testa, I.; Panico, M.; Di Stasi, R.; Caracò, C.; Tarallo, L.; Arra, C.; Barbieri, A.; Romanelli, A.; Aloj, L. *Biopolymers* **2008**, *90*, 707.
[20]. García Garayoa, E.; Schweinsberg, C.; Maes, V.; Rüegg, D.; Blanc, A.; Bläuenstein, P.; Tourwé, D. A.; Beck-Sickinger, A. G.; Schubiger, P. A. Q. *J. Nucl. Med. Mol. Imaging* **2007**, *51*, 42.
[21]. Psimadas, D.; Fani, M.; Zikos, C.; Xanthopoulos, S.; Archimandritis, S. C.; Varvarigou, A. D. *Appl. Radiat. Isot.* **2006**, *64*, 151.
[22]. Liu, S.; Hsieh, W.-Y.; Jiang, Y.; Kim, Y.-S.; Sreerama, S. G.; Chen, X.; Jia, B.; Wang, F. *Bioconjug. Chem.* **2007**, *18*, 438.
[23]. Decristoforo, C.; Faintuch-Linkowski, B.; Rey, A.; von Guggenberga, E.; Rupprich, M.; Hernandez-Gonzales, I.; Rodrigo, T.; Haubner, R. *Nucl. Med. Biol.* **2006**, *33*, 945.
[24]. Jia, B.; Liu; Z; Zhu, Z.; Shi, J.; Jin, X.; Zhao, H.; Li, F.; Liu, S.; Wang, F. *Mol. Imaging Biol.* **2011**, *13*, 730.
[25]. Shi, J.; Wang, L.; Kim, Y. S.; Zhai, S.; Liu, Z.; Chen, X.; Liu, S. *J. Med. Chem.* **2008**, *51*, 7980.
[26]. Janssen, M. L.; Oyen, W. J.; Dijkgraaf, I.; Massuger, L. F.; Frielink, C.; Edwards, D. S.; Rajopadhye, M.; Boonstra, H.; Corstens, F. H.; Boerman, O. C. *Cancer Res.* **2002**, *62*, 6146.
[27]. Haubner, R.; Bruchertseifer, F.; Bock, M.; Kessler, H.; Schwaiger, M.; Wester, H. J. *Nuklearmedizin* **2004**, *43*, 26.
[28]. Taherian, A.; Li, X.; Liu, Y.; Haas, T. A. *BMC Cancer* **2011**, *11*, 293.
[29]. Zikos, C. C.; Livaniou, E.; Leondiadis, L.; Ferderigos, N.; Ithakissios, D. S.; Evangelatos, G. P. *J. Pept. Sci.* **2003**, *9*, 419.
[30]. McCusker, C. F.; Kocienski, P. J.; Boyle, F. T.; Schatzlein, A. G. *Bioorg. Med. Chem. Lett.* **2002**, *12*, 547.
[31]. Hyde, R. D.; Jone, N. F. *Br. J. Haematol.* **1962**, *8*, 283.
[32]. Loudos, G.; Majewski, S.; Wojcik, R.; Weisenberger, A.; Sakellios, N.; Nikita, K.; Uzunoglu, N.; Bouziotis, P.; Xanthopoulos, S.; Varvarigou, A. *IEEE Trans. Nucl. Sci.* **2007**, *54*, 454.
[33]. Bullok, K. E.; Dyzlewski, M.; Prio, J. L.; Pica, C. M.; Sharma, V.; Piwnica-Worms, D. *Bioconjug. Chem.* **2002**, *13*, 1226.
[34]. Langer, M.; La Bella, R.; Garcia-Garayoa, E.; Beck-Sickinger, A. G. *Bioconjug. Chem.* **2001**, *12*, 1028.
[35]. Stichelberger, A.; Waibel, R.; Dumas, C.; Schubiger, P. A.; Schibli, R. *Nucl. Med. Biol.* **2003**, *30*, 465.
[36]. Dijkgraaf, I.; Kruijtzer, J. A.; Frielink, C.; Corstens, F. H.; Oyen, W. J.; Liskamp, R. M.; Boerman, O. C. *Int. J. Cancer* **2007**, *120*, 605.
[37]. Decristoforo, C.; Santos, I.; Pietzsch, H. J.; Kuenstler, J. U.; Duatti, A.; Smith, C. J.; Rey, A.; Alberto, R.; Von Guggenberg, E.; Haubner, R. Q. *J. Nucl. Med. Mol. Imaging* **2007**, *51*, 33.
[38]. Chen, X.; Park, R.; Tohme, M.; Shahinian, A. H.; Bading, J. R.; Conti, P. S. *Bioconjug. Chem.* **2004**, *15*, 41.
[39]. Qu, T.; Wang, Y.; Zhu, Z.; Rusckowski, M.; Hnatowich, D. J. *Nucl. Med. Commun.* **2001**, *22*, 203.
[40]. Banerjee, S. R.; Maresca, K. P.; Francesconi, L.; Valliant, J.; Babich, J. W.; Zubieta, J. *Nucl. Med. Biol.* **2005**, *32*, 1.
[41]. Fani, M.; Psimadas, D.; Zikos, C.; Xanthopoulos, S.; Loudos, G. K.; Bouziotis, P.; Varvarigou, A. D. *Anticancer Res.* **2006**, *26*, 431.
[42]. Chen, X.; Park, R.; Shahinian, A. H.; Bading, J. R.; Conti, P. S. *Nucl. Med. Biol.* **2004**, *31*, 11.
[43]. Haubner, R.; Weber, W. A.; Beer, A. J.; Vabuliene, E.; Reim, D.; Sarbia, M.; Becker, K.-F.; Goebel, M.; Hein, R.; Wester, H.-J.; Kessler, H.; Schwaiger, M. *PLOS Med.* **2005**, *70*, 244.
[44]. Alves, S.; Paulo, A.; Correia, J.; Gano, L.; Smith, C. J.; Hoffman, T. J.; Santos, I. *Bioconjug. Chem.* **2005**, *16*, 438.